

Factors Influencing Hydride Formation in a Pd/TiO₂ Catalyst

Jacinto Sá,[†] Geomar D. Arteaga,[†] Robert A. Daley,[†] Johannes Bernardi,[‡] and James A. Anderson^{*,†}

Surface Chemistry and Catalysis Group, Department of Chemistry, University of Aberdeen, Meston Walk, Old Aberdeen AB24 3UE, United Kingdom, and University Service Centre for Transmission Electron Microscopy, Technische Universität Wien, Wiedner Hauptstrasse 8-10/052, A-1040, Vienna, Austria

Received: April 9, 2006; In Final Form: June 16, 2006

A sample containing Pd nanoparticles deposited on TiO₂ was subjected to a series of different thermal pretreatments. The range of these treatments was selected to provide a palladium surface in a number of different states, including a form where TiO_x overlayers had been formed. Experiments were conducted to determine how the state of the Pd surface influenced the formation of Pd hydride. The amount of hydrogen released during a temperature-programmed experiment was used to quantify the extent of Pd β -hydride formation following room-temperature exposure to hydrogen. Samples were characterized by HAADF (high-angle annular dark-field) electron microscopy with EDX (energy-dispersive X-ray) analysis and CO pulse chemisorption and FTIR (Fourier transform infrared spectroscopy) of adsorbed CO. The amount and the ease with which Pd β -hydride was formed was found to be dependent on the metal surface area, the presence of titania overlayers, and the Pd surface roughness/defect concentration.

1. Introduction

The Pd–H₂ system is one of the most interesting metal–hydrogen systems, largely due to its relevance in hydrogenation catalysis and also as a consequence of the ability of Pd to absorb hydrogen. The use of materials with an ability to reversibly sorb hydrogen is of great interest in terms of application and role within a hydrogen economy. Hydrogen adsorption is widely used in catalyst characterization as a method of determining the average particle/crystallite size for supported metal catalysts.^{1–3} Alternative approaches include the use of transmission electron microscopy (TEM)^{4,5} and X-ray diffraction (XRD).^{6,7} However, determination of the average particle size, in certain systems, has proved to be less than straightforward. For example, in the case of reducible oxide supports, the formation of strong metal–support interactions (SMSI) leads to difficulty in determination of the true particle size due to diminished gas uptake. Inhibition of CO and H₂ chemisorption renders the use of standard volumetric experiments impracticable. In this respect, Pd/TiO₂ has already received some attention.^{8,9} Additionally Pd shows a range of different adsorbate:metal ratios as a function of particle size as evidenced by changes in the preferred CO adsorption sites (linear, bridge, 3-fold geometries) as a function of dispersion. XRD and TEM are useful techniques for the determination of average particle size, although both have limitations when dealing with very highly dispersed metals and TEM requires lengthy measurement time if results representative of the whole sample are to be obtained. Additional complications require assumptions to be made regarding particle geometry. In most cases it is assumed that the particles have a spherical shape.¹⁰

As mentioned, palladium has the ability to adsorb and absorb H₂ and several studies have been devoted to the Pd–H₂ system.^{1,2,6,7,11} In contrast to the chemisorption of H₂, where a

degree of agreement regarding adsorption stoichiometry is to be found, opinions vary regarding possible relationships between Pd particle size and hydride concentration. Most studies find that hydride concentration is enhanced by an increase in the amount of bulk-type Pd atoms, whereas other studies find that metal surface is the key factor in determining hydride concentration.

Boudart and Hwang¹ studied the solubility of hydrogen in small Pd particles supported on SiO₂ and Al₂O₃ and found an increase in the amount of sorbed hydrogen with decreasing Pd dispersion, thus confirming earlier findings of Aben.¹² However when the calculation was based on the number of bulk rather than total palladium atoms in the system (i.e., excluding the number of surface atoms), the solubility appeared to be independent of particle size. Clearly the proportion of surface atoms is significant in a highly dispersed sample, and few authors discount this number of surface atoms when calculating the number of bulk atoms and instead quote total Pd atoms in the system. In the mid-1990s, Fagherazzi et al.⁶ revisited the work of Boudart and Hwang and carried out structural studies to describe the stoichiometry between adsorbed and absorbed hydrogen in Pd/SiO₂ as a function of dispersion. Using XRD, SAXS, and temperature-programmed reduction (TPR), they found that the hydride phase concentration diminished with an increase in Pd dispersion. Discrepancies between these studies^{1,6,12} could be rationalized as a consequence of the manner by which the number of bulk Pd atoms is calculated.

Bracey and Burch² measured the quantity of hydrogen absorbed by Pd supported on SiO₂ and TiO₂ catalysts. They reported a constant ratio between hydrogen absorbed and total Pd bulk atoms for the catalysts supported on SiO₂; however, their results also demonstrated that these catalysts were quite resistant to sintering since no significant change in the amount of chemisorbed hydrogen was observed even after catalyst reduction up to 500 °C. A different scenario was reported for the Pd/TiO₂ catalysts. In this case, they observed a decrease in

[†] University of Aberdeen.

[‡] Technische Universität Wien

the ratio between hydrogen absorbed and Pd bulk atoms with an increase of the reduction temperature, which also led to a decrease in the amount of adsorbed hydrogen. The loss in the chemisorption capacity was linked to the SMSI state rather than sintering. Results would suggest a link between number of exposed Pd atoms and/or ability to adsorb hydrogen and the extent of hydride formation rather than a dependence on the number of Pd atoms displaying "bulk" metallic properties. Baker et al.⁴ showed by use of TEM and gas uptake measurements that high-temperature reduction of Pd/Al₂O₃ led to a decrease in adsorbed hydrogen due to sintering but that hydrogen absorption was not significantly affected. On the other hand, Pd/TiO₂ catalysts also underwent sintering but both adsorbed and absorbed hydrogen uptakes were affected. The authors concluded that, in the SMSI state, the presence of titanium suboxides that decorate the surface of the Pd particles inhibit both adsorbed and absorbed hydrogen states.

Flanagan and Oates¹³ have reviewed aspects of palladium–hydrogen systems. They report that, provided that Pd surface is clean, hydrogen absorption is very rapid and that the sticking coefficient is close to 1. Thus equilibration between gaseous molecular hydrogen and hydrogen dissolved in Pd should be rapidly established.

All reports indicate that changes in the Pd particle size led to changes in the fraction of absorbed (hydride) hydrogen; however, there is no agreement concerning relationship between the amount of hydride formed and the amount of exposed Pd atoms. It is also unclear as to why partial decoration of Pd by reduced titania moieties should modify the extent of hydride formation. It is expected that a methodical study of the quantification of Pd–hydride after submission of a single catalyst to different thermal treatments would be timely and might provide useful information regarding changes in the metal particle size distribution in particular, for example, for SMSI catalysts.

2. Experimental Section

2.1. Catalyst Preparation. The materials used for the synthesis of the catalysts were Pd(NO₃)₂ (Johnson Matthey) and TiO₂ (Degussa P25) with a surface area of 49 m²/g (N₂, 77 K, BET method). Pd supported on TiO₂ was synthesized by slowly dropping a solution containing the metal precursor into a constantly stirred aqueous suspension (1 g of TiO₂: 30 mL of water) of the support. The volume of liquid was dried at 60 °C for 24 h and then stirred vigorously for 2 h before a further drying process. The last step of the procedure was repeated twice to give a nominal metal loading of 2 wt %.

After synthesis, the catalysts were subjected to different calcination and reduction temperatures, which allowed different degrees of annealing and/or sintering (depending on the treatment). The pretreatment conditions were chosen to cover a range of temperatures below, between, and above the Hüttig (0.3T_M, 275 °C for Pd) and the Tammann (0.5T_M, 320 °C for Pd) temperatures.^{14,15} These temperatures are normally related to the onset of changes in the particle size. Calcination temperatures above 500 °C were avoided to prevent crystal phase transformation in the support, which would change the ratio between anatase and rutile (in P25 ~25% rutile) and surface area of the catalyst. The in situ pretreatment consisted of calcination at the desired temperature for 1 h in 20 mL/min air, reduction at desired temperature for 1 h in 5% H₂/N₂ (20 mL/min) and purging for 30 min at 200 °C under a flow of 20 mL/min N₂.

2.2. Characterization. **2.2.1. TPR Experiments.** Temperature-programmed experiments to determine hydride concentrations

were conducted on a TPD/R/O 1100 (CE instruments), equipped with a thermal conductivity detector (TCD). The experiments consisted of exposure of the sample to a flow of 5% H₂/N₂ (20 mL/min) at 20 °C for 1 h and then heating to 300 °C at 10 °C/min. The Pd–hydride concentration was determined by integration of the negative peak observed in the TPR profiles in the region 60–100 °C.^{16,17} The samples (ca. 100 mg) had been previously pretreated at a range of different calcination/reduction temperatures.

2.2.2. CO Chemisorption. Pulse chemisorption (dynamic adsorption) was performed by pulsing a known volume (100 μL, STP) of CO into the reactor. The experiments were carried out in a Perkin-Elmer Autosystem XL gas chromatograph (GC) with an air-actuated valve and a TCD. The data were analyzed using TurboChrom4 software. The injection loop was held at 120 °C within the GC/TCD oven. The CO passing through the reactor passes through a molecular sieve before passing over the TCD. The air-actuated valve was programmed to pulse CO every 10 min. The CO chemisorption analysis ran for 300 min and the pulsing was commenced after sufficient time to allow baseline stabilization.

The chemisorption of CO was also followed by diffuse reflectance infrared Fourier transform spectroscopy (DRIFT). Spectra (4 cm⁻¹ resolution, 100 scans, MCT detector) were recorded for ca. 75-mg samples in a Harrick environmental cell. The catalysts were treated in situ by the same procedure as described for the TPR measurements. CO adsorption experiments consisted of pulsing regularly (every 10 min) 0.378 mL of pure CO into a stream of N₂ (20 mL/min). The procedure was repeated until the intensity of the bands remained constant. The samples were purged afterward with nitrogen (20 mL/min) for ca. 15 min to remove gaseous and weakly adsorbed forms of CO. Spectra recorded in (diffuse) reflectance mode were converted to Kubelka–Munk (KM) by use of the spectrometer software and are presented in this manner.

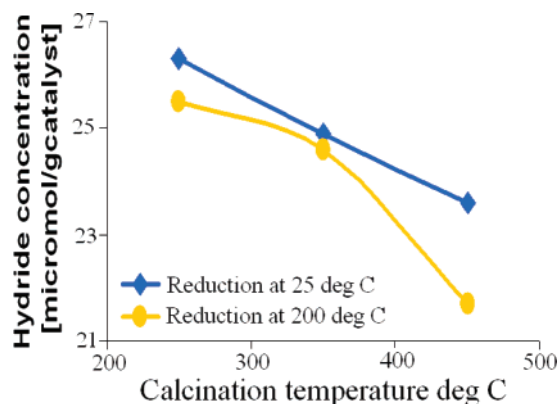
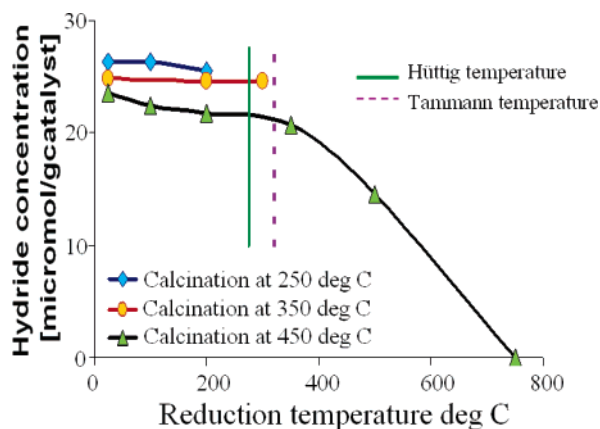
2.2.3. HAADF with EDX. Electron microscopic studies were performed on a TECNAI F20 field emission microscope equipped with a Gatan Image Filter (GIF 2001) operated at 120 or 200 kV. Electron transparent samples were prepared by drying a suspension of material in methanol on a copper grid coated with a carbon film. HAADF images are formed by collecting high-angle scattered electrons with an annular dark-field detector in a dedicated scanning transmission electron microscopy (STEM) instrument.

3. Results

TPR experiments were carried out to determine the influence of the pretreatment (calcination and/or reduction) temperature on the Pd β-hydride concentration. By varying the pretreatment's temperature, different degrees of annealing and/or sintering may be achieved, leading to changes in the particle morphology. The results obtained are summarized in Table 1. In general, low-temperature treatments give values that show limited sensitivity to temperature, whereas high reduction temperatures progressively led to a total loss of hydride. The influence of the individual effects of calcination and reduction temperature on the hydride concentration is illustrated in Figures 1 and 2, respectively. Figure 1 shows the influence of the calcination temperature, at two fixed reduction temperatures, on the amount of hydride formed. The two reduction temperatures selected were 25 and 200 °C. For both reduction temperatures, an increase in calcination temperature led to a decrease in the quantity of hydride present in the catalysts, the effect being slightly more pronounced when the catalyst was submitted to

TABLE 1: Summary of Pd Hydride Concentration as a Function of Different Pretreatment Conditions

catalyst Pd/TiO ₂ treatment	calcination temp (°C)	reduction temp (°C)	amount of Pd β -hydride ($\mu\text{mol/g}$ of catalyst)
A	250	25	26.3
B	250	100	26.3
C	250	200	25.5
D	350	25	24.9
E	350	200	24.6
F	350	300	24.6
G	450	25	23.6
H	450	100	22.4
I	450	200	21.7
J	450	350	20.7
K	450	500	14.6
L	450	750	nd ^a

^a Not detectable.**Figure 1.** Changes in the hydride concentration for Pd/TiO₂ as a function of the calcination temperature at two different fixed reduction temperatures.**Figure 2.** Changes in the hydride concentration for Pd/TiO₂ as a function of the reduction temperature at three different fixed calcination temperatures.

the higher reduction temperature. The differentiation became more significant as the calcination temperature was increased. The influence of reduction temperature at three fixed calcination temperatures is indicated in Figure 2. Figure 2 also emphasizes the temperatures that correspond to the Hüttig and Tammann temperatures for Pd. A significant, continual decrease in hydride concentration is observed when the reduction temperature is increased above 350 °C.

There are notable changes in the hydride concentration as a function of pretreatment temperature, consistent with the fact that the extent of hydride formation is sensitive to the particle size and/or morphology. However, changes only become truly significant when the catalyst was reduced above the Tammann

TABLE 2: Summary of CO Uptake, Dispersion, Average Estimated Particle Diameter, and Ratio of Bridged to Linear CO Band Intensity from FTIR as a Function of Different Pretreatment Conditions

catalyst Pd/TiO ₂ treatment	CO uptake ($\mu\text{mol/g}$ of catalyst)	dispersion (%)	particle diameter (nm)	CO band ratio bridge/linear
A	10.3	11.0	10.3	8.6
B	13.6	14.4	7.8	6.5
C	22.3	23.8	4.75	5.0
D	20.8	22.2	5.1	8.2
E	22.3	23.8	4.75	7.2
F	23.9	25.8	4.45	4.9
G	19.6	20.8	5.4	7.8
H	21.1	22.4	5.05	10.5
I	23.9	23.4	4.45	6.5
J	15.2	16.2	7.0	4.7
K	11.6	12.3	9.1	
L	nd ^a			

^a Not detectable.

temperature,¹⁴ a condition under which the metal particles acquire mobility. Note that an increase in temperature leads to an increase in the vibrational (kinetic) energy of the atoms, and above a certain critical level, these atoms become mobile. The Hüttig temperature indicates the temperature at which the atoms are mobile within the particle, whereas the Tammann temperature refers to the temperature at which the whole metal ensemble exhibits mobility.

The other goal of this work was to investigate the viability of using hydride concentration as a reliable indicator of exposed metal surface area in catalysts that are liable to experience SMSI, instead of the well-established chemisorption experiments such as CO pulse chemisorption.^{1-3,18}

Table 2 summarizes the CO uptakes of the catalysts after similar treatments as carried out in the determination of the hydride concentrations, as well as calculated average particle sizes and Pd dispersions estimated from the respective uptakes. The average particle size and Pd dispersions were calculated by use of the mathematical relation described elsewhere,¹⁹ with the assumption of a 1:2 CO:Pd ratio¹⁸ and a spherical particle shape.¹⁰ The average particle sizes calculated from the CO pulse are spread over a broad range of values. Furthermore, the results show no trend as a function of the changes in the pretreatment temperature. Low chemisorption values (and consequently large estimated particle sizes) were obtained for low reduction temperatures, possibly due to the inability to remove products of reduction (i.e., water) or other contaminants. High-temperature pretreatments also give the impression of lowering dispersion and increasing particle size. There is no correlation between hydride quantity and particle size as predicted by CO chemisorption. This is clearly depicted in Figure 3. While the hydride concentration decreases significantly only above the Tammann temperature when the Pd particles gain mobility, that is, pretreated at temperatures above 320 °C; the particles size calculated from the CO adsorption experiments show no real correlation when plotted as a function of the treatment temperature. This may be a result of combination of factors such as the presence of the SMSI state and/or multiple adsorption geometries of CO adsorption on Pd.

FTIR experiments were carried out with the objective of identifying the presence of the multiadsorption geometries under the experimental conditions adopted. Figure 4 shows the FTIR spectra after exposure to CO at room temperature. The spectra show the presence of three main forms of adsorbed CO on Pd. The band between 2100 and 2055 cm⁻¹ is due to terminal CO

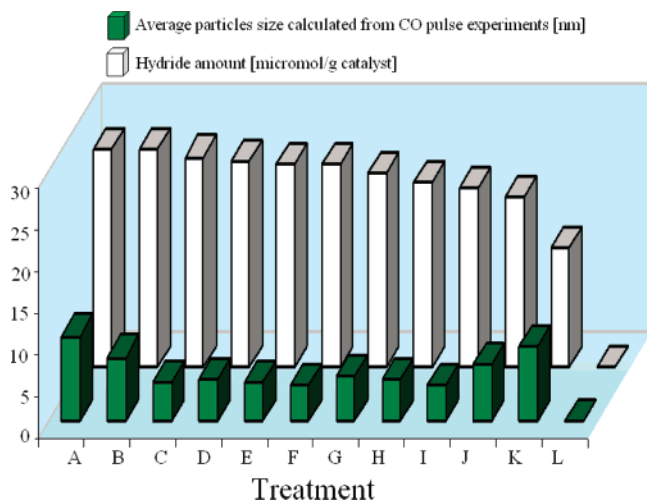


Figure 3. Comparison of average particle size calculated from the CO pulse experiments and the amount of hydride.

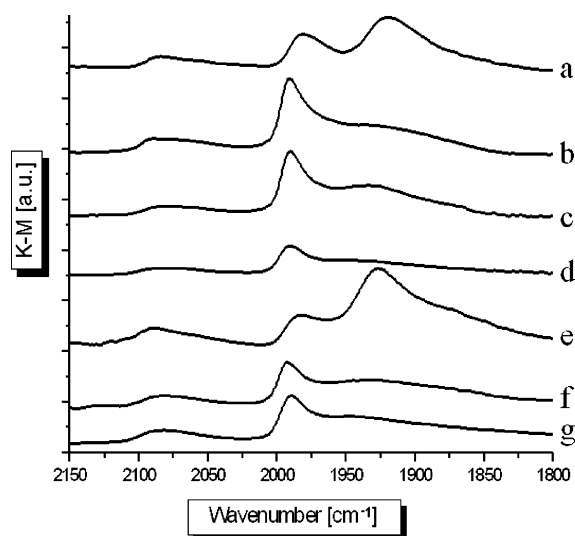


Figure 4. FTIR spectra of Pd/TiO₂ P25 after CO adsorption at room temperature with different pretreated samples: (a) treatment A; (b) treatment C; (c) treatment E; (d) treatment F; (e) treatment G; (f) treatment I; (g) treatment J.

on Pd, corresponding to a 1:1 CO:Pd ratio;^{20–23} the band between 2000 and 1975 cm^{−1} can be attributed to bridged CO on open (100) type facets (CO:Pd = 1:2) or compressed bridge CO on Pd (CO:Pd = 2:3);^{21–24} and the third band between 1950 and 1910 cm^{−1} can be assigned to isolated bridged CO on Pd (CO:Pd = 1:2).^{21–25} After certain pretreatments, such as treatment C, it was possible to identify a fourth band between 1900 and 1800 cm^{−1} that is generally assigned to CO adsorbed at 3-fold hollow sites (CO:Pd = 1:3).^{23,25,26} The ratio between the bridged (i.e., all absorption bands not representing 1:1 adsorption stoichiometry) and terminal CO on Pd are reported in Table 2, except for the samples submitted to treatments K and L. The FTIR experiments demonstrate that results from CO pulse chemisorption cannot be employed directly to calculate Pd dispersion without a careful consideration of the variation in the adsorption stoichiometry. This stoichiometry varies significantly with different pretreatments and also shows no specific trends as a function of severity of pretreatment and reduced overall uptake. The use of an arbitrary 1:2 stoichiometry here as proposed to hold over a wide range of dispersions²⁷ is equally inadequate in encompassing the full range of dispersion and surface geometries.

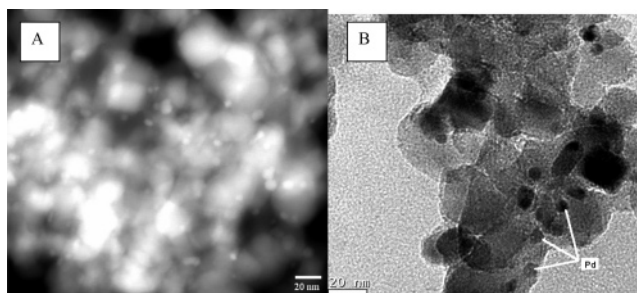


Figure 5. HAADF (A) and HR-TEM (B) images of Pd/TiO₂ after treatment J.

TEM measurements were performed to independently determine particle size without the need to rely on arbitrary adsorption or absorption stoichiometries. Figure 5 shows a representative HAADF image of Pd/TiO₂ catalyst having undergone treatment J (450 °C calcination, 350 °C reduction). The particle diameters from a number of images were found to lie in the range 5–9 nm. For this particular treatment, this range encompasses the value (7 nm) obtained from CO chemisorption by use of the arbitrary 1:2 adsorption stoichiometry (Table 2), although this is not the case for all sample treatments.²⁸

4. Discussion

The present study confirms and then extends findings regarding the formation of hydride phase for titania-supported Pd catalysts.^{2,11} Increasing the reduction temperature beyond a certain point leads to loss in the quantities of both adsorbed and absorbed gases.

Although loss of chemisorbed amounts (Table 2) may be partially justified in terms of increased particle sizes (sintering) as the pretreatment temperatures are extended beyond the Hüttig/Tammann temperatures for Pd, the corresponding but more dramatic loss in the amount of hydride formed for samples pretreated above these temperatures (Figure 2) is not consistent with the idea that the solubility of hydrogen drops to zero only when the dispersion approaches 100%.¹ The dispersions calculated by CO chemisorption (Table 2) and confirmed by particle size determination via TEM (Figure 5) for samples reduced above 350 °C indicate that diminished levels of hydride formed at and above this pretreatment temperature (Figure 2) can be attributed¹ neither to complete loss of dispersion nor to complete blockage of the Pd surface and elimination of adsorption centers. However, the recent report that reduced, crystalline titania phases are mobile and lead to partial decoration of Pd in Pd/TiO₂ catalysts at temperatures as low as 350 °C²⁸ suggests that not only are Pd atoms and particles mobile above this temperature but so too is the support phase, which must be considered as playing a role in the progressively diminished hydride levels detected for catalysts reduced above this temperature (Figure 2). Pd sites must still be available under these conditions as confirmed by the CO uptake levels, and so potential sites for adsorption and subsequently absorption must be available.

The criterion for establishing thermodynamic equilibrium between gaseous hydrogen and bulk hydride is based upon the equating of the hydrogen atom chemical potential in both phases. Although this should be independent of the amount of exposed surface, thermodynamic equilibrium can be achieved only if the surface is in a state where hydrogen dissociation can occur efficiently. It is therefore more appropriate to examine the system in terms of two separate equilibrium processes, one between gaseous and adsorbed (dissociated) states and the other

between the adsorbed surface state and the bulk hydride. In principle, a palladium surface partially covered by reduced titania entities should, from the point of view of a physical blocking perspective, still allow equilibrium to be established. However, it is clear that the state of the surface is highly relevant to the observations made in this study regarding levels of bulk hydride formed.

Since hydrogen is administered via the gas phase, the Pd surface should be sufficiently clean as to ensure the dissociation of the molecule to produce hydrogen atoms.¹³ A Pd surface free of contaminants was an important requirement for the effective formation of the hydride phase, as nonreproducible levels were determined in experiments where samples were reduced at lower temperatures (25 and 100 °C) and subsequently purged under nitrogen at the same temperature (results not shown) instead of at a fixed purge temperature of 200 °C (Table 1). The presence under these conditions of physisorbed water generated during reduction but not removed under the low purge temperatures led to a decrease in levels of hydride formation due to blockage of Pd sites required for the activation of hydrogen. That is, exposure of the surface at room temperature failed to activate hydrogen effectively when in the presence of other competitive adsorbates. The presence of water vapor in the atmosphere also inhibits the desorption of hydrogen from Pd.²⁹ Exposure to adsorbates such as CO with higher adsorption enthalpies than hydrogen were able to competitively adsorb under these conditions, for example, in FTIR or pulse chemisorption measurements, which might create the impression that surface site blockage was not responsible for the lack of hydride generated.

Reduction of the catalyst above 350 °C clearly reduces the propensity to form bulk hydride even though surface Pd sites remain exposed within the TiO_x-dominated surface layer and are capable of adsorbing CO. One might argue that, from a purely statistical basis, a reduction in the ratio of exposed surface Pd sites to bulk sites should kinetically hinder the formation of bulk hydride phase. However, given that the diffusion constant of hydrogen in bulk Pd is expected³⁰ to be on the order of 10^{-6} cm² s⁻¹ or more specifically 5.4×10^{-7} cm² s⁻¹ at the temperature of the measurements conducted here,³⁰ one could envisage that hydrogen sorption kinetics is dominated by the diffusion rate of atomic hydrogen from the surface to the subsurface/bulk layers. Other processes involved in establishing equilibrium are considerably faster; for example, the rate at which hydrogen molecules impinge upon the surface under our conditions can be calculated as 5.45×10^{23} cm⁻² s⁻¹ so that the time required to produce monolayer coverage is a fraction of a second, even if the sticking coefficient were relatively low. The sticking coefficient of hydrogen on clean palladium under the low-pressure hydrogen conditions employed here, however, is close to 1.¹³ These considerations would suggest that the system rapidly reaches a steady state in terms of the surface-adsorbed hydrogen state and, consistent with the results of Kay et al.,³¹ suggest that hydrogen absorption is bulk-diffusion-limited. However, such a scenario would not account for the reduced levels of bulk hydrogen as the number of surface-available Pd atoms was diminished.

Application of the steady-state approximation, if it is assumed that the level of adsorbed hydrogen remains constant, would predict that the rate of hydride formation is governed by the partial pressure of molecular hydrogen in the gas phase. The latter parameter was maintained constant in all experiments, as was the time allowed for equilibration between the gaseous and absorbed states. However, when this time was extended, the

amount of hydrogen that could be absorbed was increased. For example, for catalyst calcined at 450 °C and reduced at 500 °C, if the time of exposure to hydrogen at 20 °C was increased from 1 to 6 h, an increase in the amount of hydride by ca. 5.6–20.2 μmol/g was found. It is clear that the presence of the SMSI-induced TiO_x layer, kinetically hinders the establishment of equilibrium between gaseous and absorbed hydrogen. In this respect, the concentration of surface hydrogen becomes important. The relatively low values of the diffusion constant^{30,31} reflect only the transfer of hydrogen atoms between octahedral interstitial sites within palladium, whereas a more appropriate term is Fick's diffusion constant, as this provides a direct link to the concentration gradient of hydrogen at the surface/subsurface layers. Low surface hydrogen concentration arising for the presence of TiO_x overlayers becomes directly implicated in determining the rate at which the bulk hydrogen phase is formed. The underlying reason for this may be extrapolated from recent STM studies using Pd (111),³² where application of a potential at the surface led to rapid diffusion of hydrogen atoms from the bulk to the subsurface layer which, due to surface electronic density redistribution and Pd atom top-layer relaxation, made surface hydrogen states less stable than subsurface states. It is generally accepted that these subsurface states are thermodynamically more stable than bulk hydride states.³¹ While the magnitude of sample bias generated by the STM tip is far beyond that expected due to charge transfer involving the reduced titania overlayers and the nanoparticulate Pd, the effect is still likely to be manifested, even to a much lesser degree, by a lower fraction of adsorbed hydrogen atoms, and thus kinetic limitations of transfer of hydrogen atoms into the bulk. It has long been argued that noble metals supported on titania experience electronic effects.³³

In addition to the influence of the number and electronic nature of exposed surface Pd atoms in determining the ease by which bulk hydride is formed, the geometric nature of the site is also likely to be influential. Theory suggests that vacancies, for example, should act as strong trapping sites for hydrogen,³⁴ although there is less experimental evidence to suggest that defects may contribute to enhanced hydrogen solubility.¹³ Results in Figure 1, where the reduction temperature of 200 °C avoids²⁹ the formation of SMSI-induced TiO_x overlayers, show that an increase in calcination temperature from 350 to 450 °C led to decreased levels (by 2.9 μmol g⁻¹) of hydride formation, even though the relative amounts of adsorbed CO are similar after both pretreatments (22.3 vs 23.9 μmol/g). These changes in ability to form hydride may be understood on the basis of differences in the nature of the exposed surface sites as reflected in the subtle differences in the FTIR spectra of adsorbed CO (Figure 4) and as indicated by differences in the proportions of the relative bonding modes of CO (Table 2). These differences suggest that the increased calcination temperature influences the coordination on the exposed Pd atoms, probably increasing the coordination number and providing a surface with fewer steps and edge sites. Differences between levels of hydride formation following low-temperature hydrogen or air/hydrogen (Figures 1 and 2) suggest that the final morphology of the surface is a consequence of pretreatment conditions (reactive gases, etc.) rather than merely temperature. It is envisaged that loss of defect sites is detrimental to the hydride formation process, although just as in the case of the TiO_x-covered surfaces, this reflects changes to the rate of formation rather than the final equilibrium state.

5. Conclusions

Results presented here for Pd/TiO₂ indicate that the hydride concentration depends on the nature of the exposed palladium surface, including the concentration of surface defect sites, the presence of surface contaminants such as water, and the coverage of support overlayers formed by high-temperature reduction. Under these conditions, and where time is insufficient to allow equilibrium to be established, the metal surface area and quality of the exposed metal is more important than the Pd bulk volume in determining the amount of Pd hydride formed. Under these conditions, attempts to determine Pd dispersion from the amount of hydride formed would prove futile.

Acknowledgment. We appreciate the financial support from the School of Engineering & Physical Sciences of the University of Aberdeen and the Society of Chemical Industry (SCI).

References and Notes

- (1) Boudart, M.; Hwang, H. S. *J. Catal.* **1975**, *39*, 44.
- (2) Bracey, J. D.; Burch, R. *J. Catal.* **1984**, *86*, 384.
- (3) Melendrez, R.; Del Angel, G.; Bertin, V.; Valenzuela, M. A.; Barbier, J. *J. Mol. Catal. A* **2000**, *157*, 143.
- (4) Baker, R. T. K.; Prestidge, E. B.; McVicker, G. B. *J. Catal.* **1984**, *89*, 422.
- (5) Sá, J.; Vinek, H. *Appl. Catal. B* **2004**, *57*, 247.
- (6) Fagherazzi, G.; Benedetti, A.; Polizzi, S.; Di Mario, A.; Pinna, F.; Signoreto, M.; Pernicone, N. *Catal. Lett.* **1995**, *32*, 293.
- (7) Pinna, F.; Menegazzo, F.; Signoreto, M.; Canton, P.; Fagherazzi, G.; Pernicone, N. *Appl. Catal. A* **2001**, *219*, 195.
- (8) Tauster, S. J.; Fung, S. C.; Garten, R. L. *J. Am. Chem. Soc.* **1978**, *100*, 170.
- (9) Tauster, S. J.; Fung, S. C. *J. Catal.* **1978**, *53*, 29.
- (10) Marshall, R.; Webb, G.; Jackson, S. D.; Lennon, D. *J. Mol. Catal. A* **2005**, *226*, 227.
- (11) Baker, R. T. K.; Prestidge, E. B.; McVicker, G. B. *J. Catal.* **1984**, *89*, 422.
- (12) Aben, P. C. *J. Catal.* **1968**, *10*, 224.
- (13) Flanagan, T. B.; Oates, W. A. *Annu. Rev. Mater. Sci.* **1991**, *21*, 269.
- (14) Rodríguez, N. M.; Oh, S. G.; Dalla-Betta, R. A.; Baker, R. T. K. *J. Catal.* **1995**, *157*, 676.
- (15) Ruckenstein, E.; Pulvermacher, B. *AIChE J.* **1973**, *192*, 356.
- (16) Melendrez, R.; Del Angel, G.; Bertin, V.; Valenzuela, M. A.; Barbier, J. *J. Mol. Catal. A* **2000**, *157*, 143.
- (17) Batista, J.; Pintar, A.; Mandrino, D.; Jenko, M.; Martin, V. *Appl. Catal. A* **2001**, *206*, 113.
- (18) Anderson, J. A.; Fernandez-García, M. *Supported Metals in Catalysis*; Imperial College Press: London, 2004; Vol. 5.
- (19) Software Suite for TPD/R/O 1100, Instruction Manual, Thermo Finnigan.
- (20) Kang, J. H.; Shin, E. W.; Kim, W. J.; Park, J. D.; Moon, S. H. *J. Catal.* **2002**, *208*, 31.
- (21) Hadjivanov, K. I.; Vayssilov, G. N. *Adv. Catal.* **2002**, *47*, 307.
- (22) Tessier, D.; Rakai, A.; Bozon-Verduraz, F. *J. Chem. Soc., Faraday Trans.* **1992**, *88*, 741.
- (23) Sá, J.; Berger, T.; Föttinger, K.; Riss, A.; Anderson, J. A.; Vinek, H. *J. Catal.* **2005**, *234*, 282.
- (24) Choi, K.; Vannice, M. A. *J. Catal.* **1991**, *127*, 465.
- (25) Palazov, A.; Chang, C. C.; Kokes, R. J. *J. Catal.* **1975**, *36*, 338.
- (26) Amalric-Popescu, D.; Bozon-Verduraz, F. *Catal. Today* **2001**, *70*, 139.
- (27) Canton, P.; Fagherazzi, G.; Battagliarin, M.; Menegazzo, F.; Pinna, F.; Pernicone, N. *Langmuir* **2002**, *18*, 6530.
- (28) Sá, J.; Bernardi, J.; Anderson, J. A. **2006** (submitted for publication to *Langmuir*).
- (29) Wei, I.-Y.; Brewer, J. *AMP J. Technol.* **1996**, *5*, 49.
- (30) Lin, K.-W.; Chen, H.-I.; Lu, C.-T.; Tsai, Y.-Y.; Chuang, H.-M.; Chen, C.-Y.; Liu, W.-C. *Semiconductor Sci. Technol.* **2003**, *18*, 615.
- (31) Kay, B.; Peden, C.; Goodman, D. W. *Phys. Rev. B* **1986**, *34*, 817.
- (32) Sykes, E. C. H.; Fernandez-Torres, L. C.; Nanayakkara, S. U.; Mantooh, B. A.; Nevin, R. M.; Weiss, P. S. *Proc. Natl. Acad. Sci.* **2005**, *102*, 17907.
- (33) Solymosi, F. *Catal. Rev.* **1967**, *1*, 233.
- (34) Nørskov, J.; Besenbacher, F. *J. Less-Common Met.* **1987**, *130*, 475.